Genome integration and excision by a new *Streptomyces* bacteriophage, ϕJoe

Paul C. M. Fogg[1,*], Joshua A. Haley[1], W. Marshall Stark[2] and Margaret C. M. Smith[1]

[1] Biology Department, University of York, York, United Kingdom. YO10 5DD

[2] Institute of Molecular, Cell and Systems Biology, University of Glasgow, Glasgow G12 8QQ.

* Corresponding Author: Dr. Paul Fogg, Biology Building, University of York, Wentworth Way, Heslington, York, United Kingdom. YO10 5DD

Email: paul.fogg@york.ac.uk, Tel: +44-1904-328825

Running Title: Genome integration and excision by bacteriophage Joe

Keywords: serine integrase, recombination directionality factor, integration vector, R4-like phage, *Streptomyces venezuelae, Streptomyces coelicolor*, mobile genetic elements, bacteriophage genetics

Abstract

Bacteriophages are the source of many valuable tools for molecular biology and genetic manipulation. In *Streptomyces*, most DNA cloning vectors are based on serine integrase site-specific DNA recombination systems derived from phage. Because of their efficiency and simplicity, serine integrases are also used for diverse synthetic biology applications. Here we present the genome of a new *Streptomyces* phage, ϕJoe, and investigate the conditions for integration and excision of the ϕJoe genome. ϕJoe belongs to the largest *Streptomyces* phage cluster (R4-like) and encodes a serine integrase. The *attB* site from *S. venezuelae* was used efficiently by an integrating plasmid, pCMF92, constructed using the ϕJoe *int/attP* locus. The *attB* site for ϕJoe integrase was occupied in several *Streptomyces* genomes, including *S. coelicolor*, by a mobile element that varies in gene content and size between host species. Serine integrases require a phage-encoded recombination directionality factor (RDF) to activate the excision reaction. The ϕJoe RDF was identified and its function was confirmed *in vivo*. Both the integrase and RDF were active in *in vitro* recombination assays. The ϕJoe site-specific recombination system is likely to be an important addition to the synthetic biology and genome engineering toolbox.

Importance

Streptomyces spp. are prolific producers of secondary metabolites including many clinically useful antibiotics. Bacteriophage-derived integrases are important tools for genetic engineering as they enable integration of heterologous DNA into the *Streptomyces* chromosome with ease and high efficiency. Recently researchers have been applying phage integrases for a variety of applications in synthetic biology, including rapid assembly of novel combinations of genes, biosensors and biocomputing. An important requirement for optimal experimental design and predictability when using integrases, however, is the need for multiple enzymes with different specificities for their integration sites. In order to provide a broad platform of integrases we identified and validated the integrase from a newly isolated *Streptomyces* phage, ϕJoe. ϕJoe integrase is active *in vitro* and *in vivo*. The specific

recognition site for integration is present in a wide range of different Actinobacteria, including *Streptomyces venezuelae*, an emerging model bacterium in *Streptomyces* research.

Introduction.

Over the past few decades, serine integrases have become widely established as tools for genome engineering and synthetic biology (1, 2). Serine integrases are phage-encoded, DNA site-specific recombinases that mediate recombination between two short (<50 bp) sequences. The integration reaction occurs during the establishment of lysogeny, during which the integrase causes a single crossover between the *attB* site on the bacterial chromosome and the *attP* site on the circularised phage genome leading to the integrated phage DNA flanked by the recombinant sites, *attL* and *attR* (1, 3). Integrase dimers bind to the two *att* sites and produce double-strand breaks with 2 bp overhangs (3, 4); the cut ends are then exchanged and the DNA backbone is re-ligated to produce the recombinant products (5). The *attL* and *attR* sites each contain reciprocal halves of the *attP* and *attB* sites (6). As integrases are unable to use *attL* and *attR* as substrates without an accessory protein, the recombination directionality factor (RDF), the integrated phage genome is stable until the RDF-encoding gene is expressed during prophage induction (3). Recombination between *attL* and *attR* is the excision reaction and is essentially the reverse of integration, releasing the phage genome and reforming *attP* and *attB*. Whilst only integrase is required to mediate integration, excision requires both integrase and the RDF. Genome engineers have exploited these systems to integrate genes of interest into a specific site on the chromosome, which can either be the endogenous *attB* or an introduced *attB* or *attP* used as a docking site (1). The simplicity of the serine integrase mediated site-specific recombination systems means that they are reliably portable to heterologous hosts where DNA can be integrated stably and in single copy.

The simple requirements of serine integrases make them amenable to a wide variety of applications. The earliest examples of this were to integrate an *attP* plasmid into a target genome containing the cognate *attB* (or *vice versa*) (7), allowing stable delivery of genes into diverse species, including bacteria (6, 8–10), mice (11), mosquitos (12) and humans (13). More complex genetic engineering approaches use integrases in *in vitro* ordered assembly of multiple DNA fragments (14, 15). *In vivo* genome manipulations can also be achieved either by iterative rounds of recombination (16, 17) or multiplexing orthogonal integrases/*att* sites (18). Integrase mediated DNA rearrangements can also be used to provide permanent genetic memory in novel types of biosensors (19, 20). Some applications, such as *post factum* modifications (15) or biocomputing (19, 21), need controlled excision and this requires integrase and its cognate RDF. The RDF binds directly to the integrase protein and is thought to induce a conformational change that allows *attL* and *attR* to be used as recombination substrates whilst inhibiting recombination of *attB* and *attP* (22, 23).

A limiting factor for the use of serine integrases for complex, multiplexed applications is the number of well-characterized integrases and, perhaps more pressingly, RDFs. Only seven integrase/RDF pairs have been characterized to date (from phages TP901-1 (24), ϕC31 (22), ϕBT1 (25), Bxb1 (23), ϕRv1 (26) and SPBc (27), and from the excisive element of *Anabaena* and *Nostoc* cyanobacteria species (28)), but many more integrases have been studied without their RDFs (1, 2, 29–31). Integrase genes are easily identified by comparative sequence analysis and, when the integrase is prophage encoded, the attachment sites can also be predicted (31). RDFs, however, are far more difficult to predict because known examples share little sequence homology, vary markedly in size and also differ in gene location in phage genomes (1). Expansion of the available arsenal of serine integrases and RDFs is desirable to enable advanced synthetic biology applications.

Phages that encode serine integrases are prevalent in Gram-positive bacteria, and in particular in Actinobacteria. Here, we describe a newly isolated *Streptomyces* phage, ϕJoe, and its serine integrase (Int) that is only distantly related to characterized integrases. ϕJoe Int is active *in vivo* in *Streptomyces* and *E. coli*, the integrase protein is readily purified and is able to carry out efficient *in vitro* recombination. We also describe the ϕJoe RDF, a 6.8 kDa protein that is able to promote excisive recombination and inhibit integration.

Materials and Methods

Growth media

Escherichia coli strains were generally grown in LB, except where otherwise noted. Antibiotics were added for selection where appropriate (apramycin: 50 µg/ml, chloramphenicol: 50 µg/ml, kanamycin: 50 µg/ml, ampicillin: 100 µg/ml). Preparation of competent cells and transformation of *E. coli* were performed as described in Sambrook *et al.*, 2001 (32). *Streptomyces* strains were grown on Mannitol Soya agar (33) supplemented with 10 mM $MgCl_2$ for plating conjugation mixtures and antibiotics, where required (apramycin: 50 µg/ml, nalidixic acid: 25 µg/ml).

Phage Isolation. The procedures for isolation, plating and titre of phage with *Streptomyces* as the isolation host are described in detail in Kieser *et al.*, 2000 (33)**.** Raw soil samples were enriched for environmental phage using *S. coelicolor* M145 as a propagation host (34). Briefly, 3 g of soil was added to 9 ml Difco^{TM} nutrient (DN) broth (BD Diagnostics, Oxford, UK) supplemented with 10 mM $CaCl_2$, 10 mM $MgSO_4$ and 0.5% glucose. *Streptomyces* spores were added to a concentration of 10^6 colony forming units/ml (cfu/ml) and incubated at 30°C with agitation for 16 h. Soil and bacteria were removed by centrifugation and filtration through a 0.45 µm filter. A dilution series of the filtrate in SM buffer (100 mM NaCl, 8.5 mM $MgSO_4$, 50 mM Tris-HCl pH 7.5, 0.01% gelatin) was plated with *S. coelicolor* spores to isolate single plaques. Phage were recovered from single, well-isolated plaques by single plaque soak outs in DN broth and re-plated with the host strain for three rounds of plaque purification. A high titre phage preparation was generated from plates inoculated with sufficient plaque forming units (pfu) to generate almost confluent lysis (33). The phage suspensions were filtered, pelleted by ultracentrifugation and resuspended in 0.5 ml SM buffer (35). The concentrated phage were further purified by caesium chloride isopycnic density gradient centrifugation (36).

Next Generation Sequencing. Phage DNA was extracted by phenol:chloroform purification (32) and the presence of pure phage DNA was confirmed by restriction digest. Phage DNA was sequenced and assembled in collaboration with Dr Darren Smith at NU-OMICS (Northumbria University). DNA was prepared for next generation sequencing on the Ilumina MiSeq platform using the Nextera XT library preparation kit (Illumina, Saffron Waldon, UK). Samples were loaded and run using a 2 × 250 cycle V2 kit. DNA samples were diluted to 0.2 ng/µl, prior to normalization and pooling. Paired end sequencing reads were provided as FASTQ files (NU-OMICS, Northumbria University, Newcastle, UK) and subjected to downstream analysis. ORF prediction and annotations were assigned using DNA master (Lawrence lab, Pittsburgh, PA), Glimmer (37) and Genemark (38). The annotated genome sequence was submitted to GenBank (accession number: KX815338).

Electron Microscopy. Purified phage were negatively stained with uranyl acetate (39) and imaged in a FEI Tecnai 12 G2 transmission electron microscope fitted with a CCD camera.

Mass Spectrometry. Whole phage samples were run into a 7 cm NuPAGE Novex 10% Bis-Tris gel (Life Technologies) at 200 V for 6 mins. The total protein band was excised and digested in-gel with 0.5 µg trypsin, overnight at 37°C. Peptides were extracted, concentrated and loaded onto a nanoAcquity UPLC system (Waters) equipped with a nanoAcquity Symmetry C_{18}, 5 µm trap (180 µm x 20 mm Waters) and a nanoAcquity HSS T3 1.8 µm C_{18} capillary column (75 µm x 250 mm, Waters). The nanoLC system was interfaced with a maXis HD LC-MS/MS system (Bruker Daltonics) with CaptiveSpray ionisation source (Bruker Daltonics). Positive ESI-MS and MS/MS spectra were acquired using AutoMSMS mode. Instrument control, data acquisition and processing were performed using Compass 1.7 software (microTOF control, Hystar and DataAnalysis, Bruker Daltonics. The collision energy and isolation width settings were automatically calculated using the AutoMSMS fragmentation table, absolute threshold 200 counts, preferred charge states: 2 – 4, singly charged ions excluded. A single MS/MS spectrum was acquired for each precursor and former target ions were excluded for 0.8 min unless the precursor intensity increased fourfold. Protein identification was performed by searching tandem mass spectra against the NCBInr database using the Mascot search program. Matches were filtered to accept only peptides with expect scores of 0.05 or better.

Plasmid Construction. Plasmids used in this study are listed in Table 1 and oligonucleotides in Table 2. General molecular biology techniques including plasmid DNA preparation, genomic DNA preparation, restriction endonuclease digestion and agarose gel electrophoresis were performed as described in Sambrook *et al.*., 2001 (32). In-fusion cloning technology (Clontech) was generally used for construction of plasmids. Polymerase chain reaction (PCR)-amplified DNA was generated using primers with Infusion tags for insertion into plasmid vectors, which had been cut with restriction endonucleases. The ϕJoe integrating plasmid, pCMF92, was created by Infusion cloning of the ϕJoe *int* gene and *attP* region, obtained by PCR with Joe Int-attP F/R primers and ϕJoe genomic DNA as a template, into the 3.1 kbp EcoRI-SphI fragment from pSET152. Plasmid pCMF91 was generated by inserting the amplified *attP* site prepared using ϕJoe genomic DNA as a template and primers Joe *attP* F/R into EcoRI linearized pSP72. The integration sites in *S. coelicolor* were named *attLsc* and *attRsc* and were amplified from *S. coelicolor* gDNA using Joe *attB1* F/R and Joe *attB2* F/R. The *attB* site from *S. venezuelae* (*attBsv*) was amplified using *S. venezuelae* gDNA with Joe *attB Sv* F/Joe *attB* R primers. All three attachment sites were inserted into EcoRI-linearized pGEM7 to produce pCMF90, 94 and 95, respectively. The reconstituted *S. coelicolor attB* sequence (*attBsc*) was prepared from two complementary oligonucleotides, Joe *attB* Recon F and Joe *attB* Recon R (Ultramer primers, IDT) that were annealed and inserted into EcoRI-linearized pGEM7 to produce pCMF97. pCMF98 contains the ϕJoe *attLsv* and *attRsv* sites in head-to-tail orientation and was isolated by transformation of an *in vitro* recombination reaction between pCMF91 (containing ϕJoe *attP*) and pCMF95 (containing *attBsv*) into *E. coli*. The *attLsv* and *attRsv* sites in pCMF98 were confirmed by Sanger sequencing (GATC Biotech Ltd, London, UK). The recombination reporter plasmid pCMF116 was constructed by PCR amplification of *lacZα* using *E. coli* MG1655 gDNA (40) as a template and Joe BzP forward and reverse primers encoding the ϕJoe *attBsv* and ϕJoe *attP*, respectively, resulting in the *attBsv* and *attP* sites flanking the *lacZα* gene in head-to-tail orientation. The amplified DNA was inserted into XmnI-linearized pACYC184. pCMF103 was constructed in the same way as pCMF116 except that Joe LzR F/R primers containing the ϕJoe *attLsv* and *attRsv* sites were used.

The integrase expression plasmid for protein purification, pCMF87, was constructed by insertion of a PCR fragment encoding the ϕJoe *int* gene, amplified from ϕJoe gDNA using primers Joe H6-Int F/R, into NcoI-linearized pEHISTEV expression vector. ϕJoe *g52*, encoding the RDF, was PCR-amplified from ϕJoe gDNA using primers Joe MBP-g52 F/R and inserted into pETFPP_2 MBP-tag expression vector linearized by PCR with CleF/R to create pCMF96. For *in vivo* recombination assays the integrase expression plasmid, pCMF107, was constructed by insertion of a PCR fragment encoding the ϕJoe *int* gene, amplified from ϕJoe gDNA using primers Joe pBAD Int F/R, into NcoI-linearized pBAD-HisA expression vector. A ϕJoe gp52 and integrase co-expression plasmid, pCMF108, was created by amplification of each gene using Joe pBAD gp52 F/R and Joe pBAD Int Co-Ex F/Joe pBAD Int R primers, respectively, and insertion of both PCR products simultaneously into pBAD-HisA. The co-expression insert from pCMF108 was subsequently PCR-amplified using Joe H6-gp52 F/Joe H6-Int R primers and transferred to NcoI-linearized pEHISTEV to produce an alternative expression vector, pCMF117.

Conjugation and integration of plasmids in *Streptomyces.* Transfer of plasmids into *Streptomyces* strains was performed according to the procedures described by Kieser *et al.*, (2000) (33). Conjugation donors were produced by introduction of plasmids into the non-methylating *E. coli* strain, ET12567, containing an RP4 derivative plasmid (pUZ8002), by transformation. Recipient *Streptomyces* spores were used at a concentration of 10^8/ml, mixed with the *E. coli* donors, plated onto mannitol soya agar supplemented with 10 mM $MgCl_2$ with no antibiotic selection and incubated at 30°C overnight. Plates containing the donor cells were overlaid with 1 ml water containing 0.5 mg nalidixic acid (for *E. coli* counterselection) and antibiotic for selection of exconjugants (apramycin) before further incubation of all plates at

30°C for three days. Integration efficiency was calculated as the number of apramycin-resistant colonies/10^8 cfu (8).

Protein Purification. *E. coli* BL21(DE3) containing the relevant expression plasmid were grown (37°C with agitation) in 500 ml 2YT medium (1.6% w/v tryptone, 1.0% w/v yeast extract, 0.5 w/v NaCl) to mid-exponential growth phase. The cultures were rapidly chilled on ice for 15 min, IPTG was added (final concentration 0.15 mM) and the cultures were further incubated (17°C, 16 h, with agitation). Cells were harvested by centrifugation, resuspended in 20 ml lysis buffer (1 M NaCl, 75 mM Tris pH 7.75, 0.2 mg/ml lysozyme, 500 U Basemuncher Endonuclease; Expedeon Ltd.) and incubated on ice (30 min). The cells were lysed by sonication and debris was removed by centrifugation (18,000 g, 5 min, 4°C). The supernatant was applied to a 5 ml HisTrap FF crude column that had been pre-equilibrated with binding buffer (20 mM sodium phosphate, 0.5 M NaCl, 20 mM imidazole, pH 7.4) on an ÄKTA pure 25 chromatography system (GE Healthcare). Bound, his-tagged protein was eluted with a step gradient of binding buffer containing 125 mM and 250 mM imidazole. Imidazole was removed from the eluted fractions by pooling the fractions containing the desired protein and applying the pooled solutions to a HiPrep 26/10 desalting column (GE Healthcare) equilibrated with imidazole-free binding buffer. Finally, the protein extracts were subjected to size exclusion chromatography on a HiLoad 16/60 Superdex column. Purified protein fractions were concentrated in a Vivaspin sample concentrator (GE Healthcare) and quantified by absorbance at 280 nm on a Nanodrop spectrophotometer (Thermo Scientific). Protein analysis was performed by denaturing acrylamide gel electrophoresis using pre-made gels (4-12% gradient acrylamide; Expedeon Ltd.); gels were stained with InstantBlue (Expedeon, Ltd.). For storage, an equal volume of 100% glycerol was added to protein samples before freezing at -80°C.

***In vitro* Assays.** Recombination reactions (final volume of 20 μl) were carried out in ϕC31 RxE buffer (10 mM Tris pH 7.5, 100 mM NaCl, 5 mM DTT, 5 mM spermidine, 4.5% glycerol, 0.5 mg/ml BSA) (41), Bxb1 RxE buffer (20 mM Tris pH 7.5, 25 mM NaCl, 1 mM DTT, 10 mM spermidine, 10 mM EDTA) (23) or TG1 RxE (as Bxb1 RxE plus 0.1 mg/ml BSA) (42). Integrase and RDF proteins were added at the concentrations indicated for each experiment. Plasmids containing the recombination substrates were used at 100ng per reaction. Reactions were either incubated at 30°C for 2 h (to reach steady state) or for specified times. Reactions were stopped by heat (10 min, 75°C), the buffer was adjusted to be compatible with restriction enzymes and the plasmids were digested with XhoI (NEB). The linearized reaction mixtures were run on a 0.8% agarose gel and the relative band intensities were measured to assess activity. Recombination efficiencies were calculated as intensity of product band(s)/sum intensity of all bands.

Bioinformatics. The ϕJoe genome was visualized using DNAplotter (43). The *attB* DNA alignment and logo consensus sequence were created with Jalview (44). Protein sequence alignments for visual presentation were produced using the Clustalw (45) program within the Bioedit suite (46). Protein alignments for phylogenetic analysis were produced using Clustal Omega (47) and maximum likelihood trees were created in Mega6 (48). The BLOSUM62 similarity matrix was used for protein alignment and annotation (49). Structural alignment of the small RDF proteins was carried out with Promals3D (50). Band densities for *in vitro* assays were measured using the FIJI GelAnalyzer module (51). Accession numbers for all sequences used here are provide in Table S2.

Results and Discussion.

Isolation of actinophage ϕJoe and genome sequence. Raw soil samples were enriched for environmental phage using *S. coelicolor* strain M145 as a propagation host. The phage chosen for further analysis, ϕJoe, is a siphovirus with a capsid diameter of 46.5 nm (SD 1.6 nm, n=9) and a long flexible tail of 199.5 nm (SD 12 nm, n = 8) with clear striations visible in most images (Fig. 1). ϕJoe is able to plaque on a broad range of *Streptomyces* hosts, producing lytic infection of seven out of nine species tested (Table 3). *Saccharopolyspora erythraea* (formerly *Streptomyces erythraeus*) and *Streptomyces venezuelae* were resistant to infection.

Genomic DNA was extracted from high titre ϕJoe suspensions (>10^{10} pfu/ml) and sequenced on the Illumina MiSeq platform with 2,542x coverage. The phage genome is 48,941 bases (Accession: KX815338) with a GC content slightly lower than the host bacteria; 65.5% compared to ~72% for most *Streptomyces* species. BLASTn was used to measure nucleotide identity for the closest relatives to ϕJoe; the generalized transducing phage ϕCAM (52) and two newly sequenced *Streptomyces* phages, Amela and Verse (Fig. S2), are 73, 76 and 76% identical, respectively, in global alignments. The ϕJoe genome contains 81 predicted open reading frames (Fig. 2), the majority of which have similar amino acid sequences to the three phages above and the well characterized R4 phage (53). Notably, similarity to ϕJoe integrase (gp53) is absent from each of the closest genome matches but is instead present in several more distantly related phages (Fig. 3), indicative of phage mosaicism (54). Specifically, ϕJoe integrase is homologous to the uncharacterized integrases from five complete phages - Lannister (78% amino acid identity), Zemyla (74%), Danzina (73%), Lika (73%) and Sujidade (73%) (Fig. 3). Comparison to known integrases suggests that the catalytic serine is likely to be at position 46 in the protein sequence (VRL**S**VFT).

Purified phage particles were submitted for shotgun LC-MS/MS analysis to determine the structural proteome. At least one peptide match was detected from fourteen ϕJoe gene products, five of which have predicted functions – Portal, Capsid, Tail Tape Measure, Scaffold, Head-Tail Adaptor (Figure 2, Table S1). The remaining nine gene products have no known function but all cluster close to the predicted structural genes within a region of the genome spanning ~21 kbp.

Characterization of ϕJoe integrase and attachment sites. For most phage-encoded integration systems, the *attP* site lies adjacent to the *int* gene encoding the integrase. The *attP* sites for serine integrases are characteristically about 45 to 50 bp in length and contain inverted repeat sequences flanking a spacer of approximately 20 bp (3, 55). Examination of the ϕJoe genome identified a candidate *attP* site located 18 bp upstream of the *int* gene. A plasmid, pCMF92, was constructed by replacing the ϕC31 *int/attP* locus from the widely used integrating vector pSET152, with the ϕJoe *int/attP* locus (Fig.S1). Integration of pCMF92 would confirm whether the integrase is functional, the nature of the *attP* site and, by rescuing the DNA flanking the integrated plasmid, the identity of the *attB* site could be deduced (Fig. 4). pCMF92 was introduced into *S. coelicolor* J1929 and *S. lividans* TK24 by conjugation and apramycin resistant colonies were obtained, but the frequencies were low (10^{-4} to 10^{-5} exconjugants/cfu) compared to other integrating vectors (10^{-2} to 10^{-3} exconjugants/cfu) (9, 18). To test whether integration was site-specific, four *S. coelicolor*:pCMF92 cell lines were amplified from independent exconjugants and the genomic DNAs were analysed by Southern blotting using a probe derived from the ϕJoe *int* gene. In the four cell lines pCMF92 had integrated into one of two different integration sites, as revealed by hybridisation of the probe to two different restriction fragments (data not shown).

We then sought to characterize the two integration sites for pCMF92 in *S. coelicolor* by rescuing the integrated plasmids along with flanking DNA into *E. coli*. In pCMF92 there is 3.9 kbp of DNA between the ϕJoe *attP* site and the PstI cleavage site that contains the plasmid origin of replication and the apramycin resistance gene (Fig. S1). Genomic DNA from two *S. coelicolor*:pCMF92 cell lines, each containing pCMF92 integrated into one of the two different integration sites, was digested with PstI endonuclease, self-ligated and introduced into *E. coli*

DH5α by transformation. The rescued plasmids were sequenced over the recombination sites to validate the nature of the ϕJoe *attP* site and to identify the chromosomal positions of the two *S. coelicolor* integration sites. The ϕJoe *attP* site was confirmed to be ≤ 50 bp and the 5' GG dinucleotide at the centre of an imperfect inverted repeat is predicted to be where the crossover occurs (Fig. 4A).

The two *S. coelicolor* integration sites for pCMF92 are located 3.9 kbp apart, separated by an apparent mobile genetic element comprising *sco2603,* encoding a putative serine integrase with 68% identity to ϕJoe integrase and two further genes (Fig. 4B). Its product, SCO2603, is 68% identical to ϕJoe integrase. We hypothesized that the ϕJoe integrating plasmid is inefficient in *S. coelicolor* because an ancestral and optimal *attB* site is occupied by the SCO2603-encoding element. The two integration sites for pCMF92 in *S. coelicolor* were therefore called *attLsc* and *attRsc* to reflect the provenance of the sites containing the mobile element. To test this hypothesis, the sequence of the ancestral *attB* site, *attBsc*, was predicted by removing the sequence between *attLsc* and *attRs*c, including the *attP* moieties that would have originated from the inserted mobile element (Fig. 4C). The reconstituted *attBsc* was used to interrogate the GenBank *Streptomyces* database for closely related extant sequences. Three species were chosen from the top ten hits returned (*S. avermitilis*, *S. albus* and *S. venezuelae*, Fig. 4D) and assayed for *in vivo* integration efficiency. *S. venezuelae* was the only host to support highly efficient integration after conjugation with pCMF92, 160-fold greater frequency than *S. coelicolor* and 1,600-fold greater than *S. lividans* (Fig. 5A). The integration frequencies for pCMF92 into *S. venezuelae* are similar to those reported for other characterized serine integrases (9, 18) and we demonstrate below that the *attB* site from *S. venezuelae, attBsv*, is indeed used efficiently by ϕJoe integrase. Plasmid pCMF92 could therefore be used as a new integrating vector for use in this newly emerging model system for *Streptomyces* research.

The *S. venezuelae attBsv* site was used as a BLASTn query to estimate the prevalence of potential ϕJoe insertion sites in sequenced species. In many instances, each half of the query sequence matched separate locations in the target genome, suggesting that ϕJoe-like *attB* sites are frequently occupied by either a prophage or a similar mobile element to that observed in *S. coelicolor* J1929. Hits were subsequently filtered for matches of at least 80% coverage with an e-value of $<1x10^{-10}$ and a bit score >75, which revealed numerous apparently unoccupied ϕJoe *attB* sites in diverse *Streptomyces*, *Kitasatospora* and *Dermacoccus* species (Fig. 4D). Generally, the *attB* site for ϕJoe and the SCO2603 integrase-encoding elements is located 74bp from the end of an ORF encoding a SCO2606-like predicted B12 binding domain-containing radical SAM protein. Insertions this close to the end of an ORF may not necessarily cause loss of function of the gene product and this could explain the prolific number of mobile elements that use this locus as an insertion site. Other than the recombination genes, the genetic content of the mobile elements located here varies markedly in different bacterial species (Fig. S2). Some *Streptomyces* strains have an almost identical SCO2603-containing genetic element to *S. coelicolor* J1929 (e.g. WM6391), others have no genes other than the recombination genes (e.g. NRRLF-5123) and some contain up to 40 kbp between the predicted *attL* and *attR* sites (Fig. S2).

ϕJoe integrase catalyses efficient *in vivo* and *in vitro* integration. In order for an integrase to have broad appeal as a bioengineering tool it must be functional in heterologous hosts. As a proof of principle, we tested the activity of ϕJoe integrase in *E. coli* by cloning the integrase gene into an arabinose-inducible expression vector, pBAD-HisA, to produce pCMF107. Meanwhile, we constructed a reporter plasmid, pCMF116, containing the *E. coli lacZα* gene flanked by ϕJoe *attBsv* and *attP* sites in head to tail orientation (Fig. S3). Both plasmids were introduced into *E. coli* TOP10 cells (Invitrogen) by co-transformation and plated on selective agar plates containing 0.2% L-arabinose and 80 µg/ml X-Gal. pBAD-HisA lacking an insert was used as a negative control. All of the transformants were white in the presence of ϕJoe *int*, indicating efficient recombination between the *attBsv* and *attP* sites leading to loss of the *lacZα* gene (Fig. 5B & S3). ϕJoe integrase and its cognate *attBsv* and *attP* sites are, therefore, active in *E. coli*.

Another key application for serine integrases is for *in vitro* combinatorial assembly of genes for optimising expression of metabolic pathways (14, 15). In this application different integrases are used to join (by recombination) specific pairs of DNA fragments tagged with their cognate attachment sites. In theory this procedure can be multiplexed to assemble many DNA fragments together using different, orthogonally acting integrases. The aim is to generate artificial operons with defined or random order. To test the suitability of ϕJoe Int for *in vitro* recombination reactions, the integrase gene was cloned into the His-tag expression vector pEHISTEV and purified after overexpression in *E. coli*. *In vitro* recombination assays were carried out with ϕJoe *attP* (pCMF91) versus each of *attBsc, attLsc, attRsc* and *attBsv* (pCMF97, pCMF90, pCMF94 and pCMF95, respectively) and using a range of ϕJoe integrase concentrations. Successful recombination between attachment sites produces a co-integrant plasmid, which can be distinguished from the substrate plasmids by a restriction digest and agarose gel electrophoresis (Fig. S3). In this assay, recombination was undetectable when *attLsc* (pCMF90) or *attRsc* (pCMF94) were used with *attP* (pCMF91) as substrates. A small amount of recombination was observed (≤2%, Fig. S4) when the reconstituted *attBsc* (pCMF97) was used with *attP* (pCMF91). However, consistent with the observations in *E. coli* and in *Streptomyces*, the *S. venezuelae attBsv* site (pCMF95) was a highly efficient substrate for recombination with the ϕJoe *attP* site. ϕJoe integrase was effective over a broad range of concentrations (50 – 1000 nM) (Fig. 5C & S4). Using 200 nM integrase, detectable recombination product was produced after ~10-15 min, and after 2 h approximately 70% of the substrate molecules were converted to product (Fig. 5C & D).

There are only 6 bp that differ between *attBsc* and *attBsv*, and all the differences are on the left-hand arm of the *attB* sites (Fig. 4C). Previously, a mutational analysis of the ϕC31 *attB* site showed that mutationally sensitive bases occur 2, 15 and 16 bases to either side of the crossover dinucleotide (56). As two of the differences between *attBsc* and *attBsv* are also 2 and 16 bases from the putative crossover 5’GG (Fig. 4C), these base pair differences might account for the poor activity of *attBsc* in the *in vitro* assays.

Identification and validation of the ϕJoe RDF protein, gp52. Although there are dozens of serine integrases that have been described in the literature, there are only seven published RDFs for serine integrases (ϕC31 gp3 (22), ϕBT1 gp3 (25), Bxb1 gp47 (23), TP901 ORF7/Xis (24), Anabaena/Nostoc XisI (57), SPBc SprB (27), and ϕRv1 Rv1584c/Xis (26))**.** The Bxb1 and ϕC31 RDFs are amongst the largest of these RDF proteins (approximately 27.5 kDa, 250 amino acids) and their genes are located in proximity to the phage DNA replication genes. Both RDFs have functions during phage replication in addition to acting as RDFs but they are evolutionarily unrelated (25, 58). The RDFs from ϕBT1 and another ϕC31-like phage, TG1, are close relatives of the ϕC31 RDF at the sequence level (85% and 59% identical, respectively); furthermore, the ϕBT1-encoded RDF acts on ϕC31 integrase and *vice versa* (25). The ϕRv1 and SPBc RDFs are located within 1 or 2 ORFs of the *int* gene, a feature which is reminiscent of the *xis* genes that act with tyrosine integrases. ϕRv1, SPBc, TP901 and Anabaena/Nostoc RDFs are much smaller proteins than ϕC31 gp3 or Bxb1 gp47 (58 and 110 amino acids). Given the variation in RDF size, sequence and genomic location, there are no sound generalizations yet for identifying new RDFs in phage genomes.

A list of four candidate genes (*g40, 43, 49* and *52*) for the ϕJoe RDF was drawn up based on comparable size to known, small RDFs and genomic location (i.e. not located amongst the late/structural genes) (Fig. 2). One of the potential RDF genes (*g52*) is adjacent to *int* in the ϕJoe genome, but it is transcribed divergently, with the *attP* site situated between *int* and *g52* (Fig. 2). Unlike the other candidate RDFs, gp52 homologues are only found in those phages with ϕJoe-like integrases (Fig. 3), and phylogenetic analysis of gp52 and the integrase indicated that both proteins have followed a parallel evolutionary path (Fig. S5). Pairwise alignment of the 6.8 kDa (62 amino acids) gp52 protein with other known small RDFs revealed homology with ϕRv1 RDF (25.7% identity and 35.1% similarity; Fig. 6A). Also, examination of the mobile elements that have inserted into the *attB* sites in *S. coelicolor* and other *Streptomyces* spp, revealed that they also contain a gene encoding a gp52 homologue in a similar genetic context i.e. the *int* and *g52* genes are adjacent to the *attL* and *attR* sites, respectively, and would flank *attP* after excision (Fig. 4B & S2). The predicted secondary structure of ϕJoe gp52 contains an alpha-helix in the N-terminal region, a beta-sheet in the C-terminal region and an unstructured region in between (Fig. S6). Alignment of the ϕJoe-like RDFs found in intact phages and the RDFs found in the SCO2603-encoding mobile elements indicated that both of the structured regions are well conserved, particularly the putative alpha-helix, but the centre of the protein is variable (Fig. S6).

RDFs are able to influence integrase-catalysed recombination in two ways; they activate the *attL* x *attR* reaction to regenerate *attP* and *attB* (excision) and they inhibit the *attB* x *attP* integration reaction (22, 23). We were unable to produce sufficient soluble gp52 protein for *in vitro* assays when expressed with a simple histidine-tag; however, a maltose-binding protein MBP-gp52 fusion protein was more soluble. We tested the ability of MBP-gp52 to inhibit integration by titrating the protein against a fixed concentration of integrase at MBP-gp52:Int ratios of 1:2 to 22.5:1. When the MBP-gp52 was in excess integration was repressed to less than 10%; however, at less than equimolar concentrations, recombination was equivalent to the control in which no MBP-gp52 was added (Fig. 6B). These results are similar to observations for ϕC31 and Bxb1 integrases and their cognate RDFs, gp3 and gp47 (22, 23).

To test the ability of gp52 to activate an excision reaction, a plasmid containing the cognate *attLsv* and *attRsv* sites was produced, pCMF98 (Fig. S3). The MBP-gp52 protein was unable to promote efficient excision under any conditions tested (not shown). Removal of the MBP-tag, using 3c protease, increased excision activity but the reaction was still inefficient after 2 h incubation (Fig. 6C). Longer incubations of 5 – 20 h further increased the amount of substrates converted to product up to 45%, but also led to significant amounts of excision products (10-20%) by the integrase alone. Thus, in comparison to the activity of other RDFs, gp52 has rather poor activity; ϕC31 gp3 activates approximately 60 to 80% conversion of the *attL* x *attR* substrates to products (22) and similar results are obtained with other RDFs (23, 25, 26).

To test the excision ability of ϕJoe gp52 *in vivo*, a *g52* and *int* co-expression operon was designed in which *int* and *g52* were located directly downstream of the T7 promoter and ribosome binding site (RBS) in the expression vector pEHISTEV to produce pCMF117. A reporter plasmid, pCMF103, was produced containing the *lacZα* gene flanked by ϕJoe *attLsv* and *attRsv* sites (Fig. S3). pCMF117 and pCMF103 were introduced into *E. coli* BL21(DE3) cells by co-transformation and plated onto LB agar supplemented with 0.5 mM IPTG to induce expression of the *g52-int* operon (30). The reporter plasmid was then extracted from the BL21(DE3) transformants and introduced into *E. coli* DH5α to determine the percentage of plasmids that had undergone *attLsv* x *attRsv* recombination and had lost the *lacZα* gene. As controls, plasmids expressing either only integrase (pCMF87) or only gp52 (pCMF100) were also introduced together with the reporter (pCMF103) into BL21(DE3) and the assay was repeated using the same procedure. When ϕJoe integrase alone was expressed, excision occurred at a frequency of 37.6% (SD=5.1%, n=5) but when co-expressed with gp52 the frequency rose to 96.8% (SD=1.3%, n=5) (Fig. 6D). Expression of gp52 without integrase led to no detectable excision events (Fig. 6D). Although overall recombination *in vivo* was higher than *in vitro*, the relative levels of *attLsv* x *attRsv* recombination by ϕJoe integrase alone and ϕJoe integrase with gp52 were comparable. Taken together, the *in vivo* and *in vitro* data indicate that ϕJoe gp52 has RDF activity.

The observation that ϕJoe integrase has a basal level of excision activity in the absence of its RDF is highly unusual for a phage-encoded integrase and further study may provide novel insights into the mechanism and evolution of the serine integrases. *Streptomyces* phage ϕBT1 integrase was shown to catalyse bidirectional recombination, albeit at extremely low levels (59). The archetypal ϕC31 integrase is only able to mediate *attL* x *attR* recombination in the absence of gp3 when certain mutations are introduced just upstream or within a motif, the coiled coil motif, required for subunit-subunit interactions during synapsis of DNA substrates (60). The coiled coil motifs are also thought to play a role in inhibiting recombination between *attL* and *attR* in the absence of the RDF; the ϕC31 IntE449K mutation or its RDF, gp3, relieves this inhibition (55, 60–62). Three independent structural predictions indicate the presence of a coiled coil domain in the ϕJoe Int C-terminal domain (A395-T453, Fig. S7). The high basal excision activity of ϕJoe integrase could be due to incomplete inhibition of synapsis by the coiled coil motif when integrase is bound to *attL* and *attR*, reminiscent of the hyperactive ϕC31 mutant IntE449K (60). Natural bidirectional, large serine recombinases include the transposases TnpX (63) and TndX (64) from clostridial integrated conjugative elements (ICEs); ϕJoe integrase could be an evolutionary intermediate between these bi-directional recombinases and the highly directional recombinases such as ϕC31 and Bxb1 integrases. Our data show that, under the *in vitro* conditions used, gp52 was highly effective at inhibiting integration by ϕJoe integrase but only weakly activated excision. It remains to be seen whether this system, with its unusual properties, is sufficiently robust to regulate phage genome integration and excision according to the developmental choices of ϕJoe.

The properties of the ϕJoe integrase and gp52 are compatible with some of the existing applications for serine integrases, but they could also present opportunities for new applications. ϕJoe integrase is highly efficient in integration assays *in vivo* and *in vitro,* and *in vivo* excision when the RDF is present. In *attB* x *attP* integration assays, the yield of products by ϕJoe integrase was comparable to well established integrases such as those of ϕC31 or Bxb1. Furthermore, ϕJoe integrase is active in buffers compatible with other characterized integrases indicating that it could be used in DNA assembly procedures in combination with other integrases. Although yet to be tested, assemblies generated with ϕJoe integrase could later be used as substrates for modification by ϕJoe integrase in a single step. The innate excision activity of ϕJoe integrase could excise a fragment flanked by *attLsv* or *attRsv* sites and, in the same reaction, replace it via an integration reaction. ϕJoe integrase could therefore provide a more streamlined tool than the existing requirement for two steps by the more directional integrases such as those from ϕC31 and Bxb1 (15). Furthermore, given that ϕJoe Int can mediate basal levels of excision in the absence of RDF, integrating plasmids based on ϕJoe *int/attP* may display a degree of instability. Selection for the plasmid marker would ensure plasmid maintenance when desired but, if the plasmid is easily lost without selection, this trait could be desirable if there is a need to cure the strain of the plasmid or during studies on synthetic lethality.

Conclusions. On the basis of sequence and genome organisation, phage Joe is a member of a large cluster of R4-like *Streptomyces* phages. Its closest relatives at the nucleotide level are *Streptomyces* phages Amila and Verse with very high levels of nucleotide identity in the regions encoding essential early and structural genes. However, Joe integrase is more closely related to the integrases from five other R4-like cluster phages - Lannister, Danzina, Zemlya, Lika and Sujidade. At the present time the majority of *Streptomyces* phages belong to the R4-like cluster phages, but there is a continuum of relatedness throughout the cluster; for example R4 is a more distant relative to ϕJoe than any of the other phages mentioned above.

We identified the RDF for Joe integrase on the basis of its gene location, small size and distant similarity to another known RDF, Rv1584c. Although this identification was relatively straightforward, it is not clear yet how general such an approach might be. The activity of ϕJoe integrase and RDF contributes to the growing number of complete serine integrase site-specific recombination systems that are available for use in synthetic biology applications. The ϕJoe *int/attP* plasmid, pCMF92, also adds to the number of useful integrating vectors for use in *Streptomyces* species. However, and unusually for a phage integrase, ϕJoe Int displays a significant level of excisive recombination in the absence of its RDF while still being efficient at mediating integration. This bi-directional property could be applied in new ways in future applications of serine integrases.

Acknowledgements

We are grateful to Dr Darren Smith (NU-OMICS, Northumbria University) for phage genome sequencing and assembly, and to the York Biosciences Technology Facility for proteomics and electron microscopy. This research was performed with funding from the Biotechnology and Biological Sciences Research Council (project grant BB/K003356/1) and the Microbiology Society (formerly Society for General Microbiology) with a Harry Smith Vacation Scholarship for JH.

References.

1. **Fogg PCM**, **Colloms S**, **Rosser S**, **Stark M**, **Smith MCM**. 2014. New applications for phage integrases. J Mol Biol **426**:2703–2716.
2. **Groth AC**, **Calos MP**. 2004. Phage integrases: Biology and applications. J Mol Biol **335**:667–678.
3. **Smith MCM**. 2015. Phage-encoded Serine Integrases and Other Large Serine Recombinases. Microbiol Spectr **3**:1–19.
4. **Smith MCA**, **Till R**, **Smith MCM**. 2004. Switching the polarity of a bacteriophage integration system. Mol Microbiol **51**:1719–1728.
5. **Olorunniji FJ**, **Buck DE**, **Colloms SD**, **McEwan AR**, **Smith MCM**, **Stark WM**, **Rosser SJ**. 2012. Gated rotation mechanism of site-specific recombination by ϕC31 integrase. Proc Natl Acad Sci U S A **109**:19661–6.
6. **Thorpe HM**, **Smith MC**. 1998. In vitro site-specific integration of bacteriophage DNA catalyzed by a recombinase of the resolvase/invertase family. Proc Natl Acad Sci U S A **95**:5505–5510.
7. **Kuhstoss S**, **Richardson MA**, **Rao RN**. 1991. Plasmid cloning vectors that integrate site-specifically in Streptomyces spp. Gene **97**:143–146.
8. **Fayed B**, **Ashford DA**, **Hashem AM**, **Amin MA**, **El Gazayerly ON**, **Gregory MA**, **Smith MCM**. 2015. Multiplexed integrating plasmids for engineering of the erythromycin gene cluster for expression in Streptomyces spp. and combinatorial biosynthesis. Appl Environ Microbiol **81**:8402–8413.
9. **Gregory MA**, **Till R**, **Smith MCM**. 2003. Integration site for Streptomyces phage ϕBT1 and development of site-specific integrating vectors. J Bacteriol **185**:5320–5323.
10. **Hong Y**, **Hondalus MK**. 2008. Site-specific integration of Streptomyces ϕC31 integrase-based vectors in the chromosome of Rhodococcus equi. FEMS Microbiol Lett **287**:63–68.
11. **Chavez CL**, **Keravala A**, **Chu JN**, **Farruggio AP**, **Cuéllar VE**, **Voorberg J**, **Calos MP**. 2012. Long-Term Expression of Human Coagulation Factor VIII in a Tolerant Mouse Model Using the φC31 Integrase System. Hum Gene Ther **23**:390–398.
12. **Meredith JM**, **Basu S**, **Nimmo DD**, **Larget-Thiery I**, **Warr EL**, **Underhill A**, **McArthur CC**, **Carter V**, **Hurd H**, **Bourgouin C**, **Eggleston P**. 2011. Site-specific integration and expression of an anti-malarial gene in transgenic Anopheles gambiae significantly reduces Plasmodium infections. PLoS One **6**:e14587.
13. **Groth AC**, **Olivares EC**, **Thyagarajan B**, **Calos MP**. 2000. A phage integrase directs efficient site-specific integration in human cells. Proc Natl Acad Sci U S A **97**:5995–6000.
14. **Zhang L**, **Zhao G**, **Ding X**. 2011. Tandem assembly of the epothilone biosynthetic gene cluster by in vitro site-specific recombination. Sci Rep **1**:141.
15. **Colloms SD**, **Merrick CA**, **Olorunniji FJ**, **Stark WM**, **Smith MCM**, **Osbourn A**, **Keasling JD**, **Rosser SJ**. 2014. Rapid metabolic pathway assembly and modification using serine integrase site-specific recombination. Nucleic Acids Res **42**.
16. **Dafhnis-Calas F**, **Xu Z**, **Haines S**, **Malla SK**, **Smith MCM**, **Brown WRA**. 2005. Iterative in vivo assembly of large and complex transgenes by combining the activities of ϕC31 integrase and Cre recombinase. Nucleic Acids Res **33**:e189.
17. **Xu Z**, **Lee NCO**, **Dafhnis-Calas F**, **Malla S**, **Smith MCM**, **Brown WRA**. 2008. Site-specific recombination in Schizosaccharomyces pombe and systematic assembly of a 400kb transgene array in mammalian cells using the integrase of Streptomyces phage ϕBT1. Nucleic Acids Res **36**:e9.
18. **Fayed B**, **Younger E**, **Taylor G**, **Smith MCM**. 2014. A novel Streptomyces spp. integration vector derived from the S. venezuelae phage, SV1. BMC Biotechnol **14**:51.
19. **Siuti P**, **Yazbek J**, **Lu TK**. 2013. Synthetic circuits integrating logic and memory in living cells. Nat Biotechnol **31**:448–52.
20. **Bonnet J**, **Subsoontorn P**, **Endy D**. 2012. Rewritable digital data storage in live cells

via engineered control of recombination directionality. Proc Natl Acad Sci **109**:8884–8889.

21. **Bonnet J**, **Yin P**, **Ortiz ME**, **Subsoontorn P**, **Endy D**. 2013. Amplifying genetic logic gates. Science (80-) **340**:599–603.

22. **Khaleel T**, **Younger E**, **Mcewan AR**, **Varghese AS**, **Smith MCM**. 2011. A phage protein that binds ϕC31 integrase to switch its directionality. Mol Microbiol **80**:1450–1463.

23. **Ghosh P**, **Wasil LR**, **Hatfull GF**. 2006. Control of phage Bxb1 excision by a novel recombination directionality factor. PLoS Biol **4**:0964–0974.

24. **Breüner A**, **Brøndsted L**, **Hammer K**. 1999. Novel organization of genes involved in prophage excision identified in the temperate lactococcal bacteriophage TP901-1. J Bacteriol **181**:7291–7297.

25. **Zhang L**, **Zhu B**, **Dai R**, **Zhao G**, **Ding X**. 2013. Control of directionality in Streptomyces phage ϕBT1 integrase-mediated site-specific recombination. PLoS One **8**:e80434.

26. **Bibb LA**, **Hancox MI**, **Hatfull GF**. 2005. Integration and excision by the large serine recombinase ϕRv1 integrase. Mol Microbiol **55**:1896–1910.

27. **Abe K**, **Kawano Y**, **Iwamoto K**, **Arai K**, **Maruyama Y**, **Eichenberger P**, **Sato T**. 2014. Developmentally-Regulated Excision of the SPβ Prophage Reconstitutes a Gene Required for Spore Envelope Maturation in Bacillus subtilis. PLoS Genet **10**:e1004636.

28. **Ramaswamy KS**, **Carrasco CD**, **Fatma T**, **Golden JW**. 1997. Cell-type specificity of the Anabaena fdxN-element rearrangement requires xisH and xisI. Mol Microbiol **23**:1241–1249.

29. **Xu Z**, **Brown WRA**. 2016. Comparison and optimization of ten phage encoded serine integrases for genome engineering in Saccharomyces cerevisiae. BMC Biotechnol **16**:13.

30. **Xu Z**, **Thomas L**, **Davies B**, **Chalmers R**, **Smith M**, **Brown W**. 2013. Accuracy and efficiency define Bxb1 integrase as the best of fifteen candidate serine recombinases for the integration of DNA into the human genome. BMC Biotechnol **13**:87.

31. **Yang L**, **Nielsen AAK**, **Fernandez-Rodriguez J**, **McClune CJ**, **Laub MT**, **Lu TK**, **Voigt CA**. 2014. Permanent genetic memory with >1-byte capacity. Nat Methods **11**:1261–1266.

32. **Sambrook J**, **Fritsch EF**, **Maniatis T**. 2001. Molecular Cloning: A Laboratory Manual. Cold Spring Harb Lab **3**:2344.

33. **Kieser T**, **Bibb MJ**, **Buttner MJ**, **Chater KF**, **Hopwood DA**. 2000. Practical Streptomyces Genetics. John Innes Cent Ltd.

34. **Bentley SD**, **Chater KF**, **Cerdeño-Tárraga a-M**, **Challis GL**, **Thomson NR**, **James KD**, **Harris DE**, **Quail M a**, **Kieser H**, **Harper D**, **Bateman a**, **Brown S**, **Chandra G**, **Chen CW**, **Collins M**, **Cronin a**, **Fraser a**, **Goble a**, **Hidalgo J**, **Hornsby T**, **Howarth S**, **Huang C-H**, **Kieser T**, **Larke L**, **Murphy L**, **Oliver K**, **O'Neil S**, **Rabbinowitsch E**, **Rajandream M**, **Rutherford K**, **Rutter S**, **Seeger K**, **Saunders D**, **Sharp S**, **Squares R**, **Squares S**, **Taylor K**, **Warren T**, **Wietzorrek a**, **Woodward J**, **Barrell BG**, **Parkhill J**, **Hopwood D a**. 2002. Complete genome sequence of the model actinomycete Streptomyces coelicolor A3(2). Nature **417**:141–147.

35. **Fogg PCM**, **Hynes AP**, **Digby E**, **Lang AS**, **Beatty JT**. 2011. Characterization of a newly discovered Mu-like bacteriophage, RcapMu, in Rhodobacter capsulatus strain SB1003. Virology, 2011/10/25 ed. **421**:211–221.

36. **Clokie MRJ**, **Kropinski AM**. 2009. BacteriophagesMethods in molecular biology.

37. **Delcher AL**, **Harmon D**, **Kasif S**, **White O**, **Salzberg SL**. 1999. Improved microbial gene identification with GLIMMER. Nucleic Acids Res **27**:4636–4641.

38. **Besemer J**, **Borodovsky M**. 2005. GeneMark: Web software for gene finding in prokaryotes, eukaryotes and viruses. Nucleic Acids Res **33.**

39. **Booth DS**, **Avila-Sakar A**, **Cheng Y**. 2011. Visualizing Proteins and Macromolecular Complexes by Negative Stain EM: from Grid Preparation to Image Acquisition. J Vis

Exp 1–8.

40. **Frederick R. Blattner * Guy Plunkett III * Craig A Bloch Nicole T Perna Valerie Burland Monica Riley Julio Collado-Vides Jeremy D Glasner Christopher K Rode George F Mayhew Jason Gregor Nelson Wayne Davis Heather A Kirkpatrick Michael A Goeden Debra J Rose Bob Mau Ying Shao**. 1997. The Complete Genome Sequence of Escherichia coli K-12. Science (80-) **277**:1453–1462.

41. **McEwan AR**, **Raab A**, **Kelly SM**, **Feldmann J**, **Smith MCM**. 2011. Zinc is essential for high-affinity DNA binding and recombinase activity of ρc31 integrase. Nucleic Acids Res **39**:6137–6147.

42. **Morita K**, **Morimura K**, **Fusada N**, **Komatsu M**, **Ikeda H**, **Hirano N**, **Takahashi H**. 2012. Site-specific genome integration in alphaproteobacteria mediated by TG1 integrase. Appl Microbiol Biotechnol **93**:295–304.

43. **Carver T**, **Thomson N**, **Bleasby A**, **Berriman M**, **Parkhill J**. 2009. DNAPlotter: Circular and linear interactive genome visualization. Bioinformatics **25**:119–120.

44. **Waterhouse AM**, **Procter JB**, **Martin DMA**, **Clamp M**, **Barton GJ**. 2009. Jalview Version 2-A multiple sequence alignment editor and analysis workbench. Bioinformatics **25**:1189–1191.

45. **Larkin M**, **Blackshields G**, **Brown N**, **Chenna R**, **McGettigan P**, **McWilliam H**, **Valentin F**, **Wallace I**, **Wilm A**, **Lopez R**, **Thompson J**, **Gibson T**, **Higgins D**. 2007. ClustalW and ClustalX version 2. Bioinformatics **23**:2947–2948.

46. **Hall T**. 1999. BioEdit: a user-friendly biological sequence alignment editor and analysis program for Windows 95/98/NT. Nucleic Acids Symp Ser **41**:95–98.

47. **Sievers F**, **Wilm A**, **Dineen D**, **Gibson TJ**, **Karplus K**, **Li W**, **Lopez R**, **McWilliam H**, **Remmert M**, **Söding J**, **Thompson JD**, **Higgins DG**. 2011. Fast, scalable generation of high-quality protein multiple sequence alignments using Clustal Omega. Mol Syst Biol **7**:539.

48. **Tamura K**, **Stecher G**, **Peterson D**, **Filipski A**, **Kumar S**. 2013. MEGA6: Molecular evolutionary genetics analysis version 6.0. Mol Biol Evol **30**:2725–2729.

49. **Pearson WR**. 2013. Selecting the right similarity-scoring matrix. Curr Protoc Bioinforma **43**:3.5.1–9.

50. **Pei J**, **Grishin N V**. 2014. PROMALS3D: Multiple protein sequence alignment enhanced with evolutionary and three-dimensional structural information. Methods Mol Biol **1079**:263–271.

51. **Schindelin J**, **Arganda-Carreras I**, **Frise E**, **Kaynig V**, **Longair M**, **Pietzsch T**, **Preibisch S**, **Rueden C**, **Saalfeld S**, **Schmid B**, **Tinevez J-Y**, **White DJ**, **Hartenstein V**, **Eliceiri K**, **Tomancak P**, **Cardona A**. 2012. Fiji: an open-source platform for biological-image analysis. Nat Methods **9**:676–682.

52. **Monson R**, **Salmond GP**. 2012. Genome sequence of a new Streptomyces coelicolor generalized transducing bacteriophage, PhiCAM. J Virol **86**:13860.

53. **McDonald JE**, **Smith DL**, **Fogg PCM**, **McCarthy AJ**, **Allison HE**. 2010. High-throughput method for rapid induction of prophages from lysogens and its application in the study of shiga toxin-encoding escherichia coli strains. Appl Environ Microbiol, 2010/02/09 ed. **76**:2360–2365.

54. **Hendrix RW**, **Smith MC**, **Burns RN**, **Ford ME**, **Hatfull GF**. 1999. Evolutionary relationships among diverse bacteriophages and prophages: all the world's a phage. Proc Natl Acad Sci U S A **96**:2192–7.

55. **Rutherford K**, **Yuan P**, **Perry K**, **Sharp R**, **Van Duyne GD**. 2013. Attachment site recognition and regulation of directionality by the serine integrases. Nucleic Acids Res **41**:8341–8356.

56. **Gupta M**, **Till R**, **Smith MCM**. 2007. Sequences in attB that affect the ability of phiC31 integrase to synapse and to activate DNA cleavage. Nucleic Acids Res **35**:3407–19.

57. **Ramaswamy KS**, **Carrasco CD**, **Fatma T**, **Golden JW**. 1997. Cell-type specificity of the Anabaena fdxN-element rearrangement requires xisH and xisI. Mol Microbiol

23:1241–1249.

58. **Savinov A**, **Pan J**, **Ghosh P**, **Hatfull GF**. 2012. The Bxb1 gp47 recombination directionality factor is required not only for prophage excision, but also for phage DNA replication. Gene **495**:42–48.

59. **Zhang L**, **Ou X**, **Zhao G**, **Ding X**. 2008. Highly efficient in vitro site-specific recombination system based on Streptomyces phage ϕBT1 integrase. J Bacteriol **190**:6392–6397.

60. **Rowley PA**, **Smith MCA**, **Younger E**, **Smith MCM**. 2008. A motif in the C-terminal domain of ϕC31 integrase controls the directionality of recombination. Nucleic Acids Res **36**:3879–3891.

61. **Rutherford K**, **Van Duyne GD**. 2014. The ins and outs of serine integrase site-specific recombination. Curr Opin Struct Biol **24**:125–131.

62. **Hwang WC**, **Golden JW**, **Pascual J**, **Xu D**, **Cheltsov A**, **Godzik A**. 2014. Site-specific recombination of nitrogen-fixation genes in cyanobacteria by XisF-XisH-XisI complex: Structures and models. Proteins Struct Funct Bioinforma n/a–n/a.

63. **Lyras D**, **Adams V**, **Lucet I**, **Rood JI**. 2004. The large resolvase TnpX is the only transposon-encoded protein required for transposition of the Tn4451/3 family of integrative mobilizable elements. Mol Microbiol **51**:1787–1800.

64. **Wang H**, **Mullany P**. 2000. The large resolvase TndX is required and sufficient for integration and excision of derivatives of the novel conjugative transposon Tn5397. J Bacteriol **182**:6577–6583.

65. **Wilkinson CJ**, **Hughes-Thomaz ZA**, **Martin CJ**, **Bohm I**, **Mironenko T**, **Deacon M**, **Wheatcraft M**, **Wirtz G**, **Stanton J**, **Leadlay PF**. 2002. Increasing the efficiency of heterologous promoter in actinomycetes. J Mol Microbiol Biotechnol **4**:417–426.

66. **Liu H**, **Naismith JH**. 2009. A simple and efficient expression and purification system using two newly constructed vectors. Protein Expr Purif **63**:102–111.

67. **Fogg MJ**, **Wilkinson AJ**. 2008. Higher-throughput approaches to crystallization and crystal structure determination. Biochem Soc Trans **36**:771–775.

68. **Coulsox AR**, **Barrell BG**. 1978. The Nucleotide Sequence of Bacteriophage. Nucleic Acids Res **16**:355.

69. **Paget MSB**, **Chamberlin L**, **Atrih A**, **Foster SJ**, **Buttner MJ**. 1999. Evidence that the extracytoplasmic function sigma factor σ^E is required for normal cell wall structure in *Streptomyces coelicolor* A3(2). J Bacteriol **181**:204–211.

Figures

Figure 1: A ϕJoe virion imaged by transmission electron microscopy.

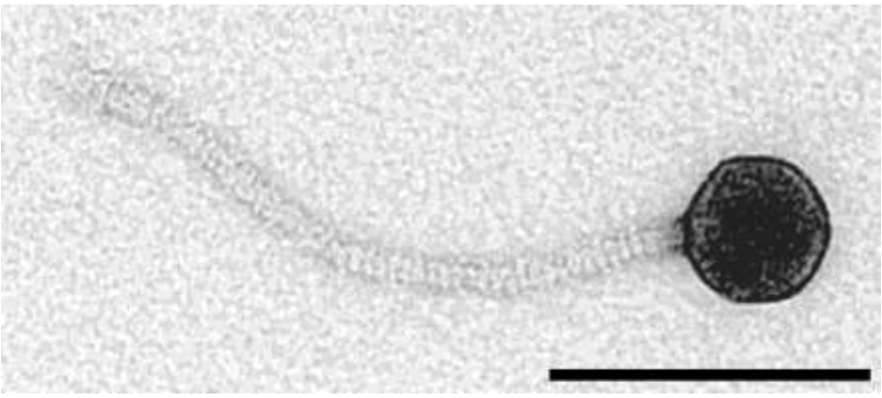

Figure 2: Schematic of the ϕJoe genome.

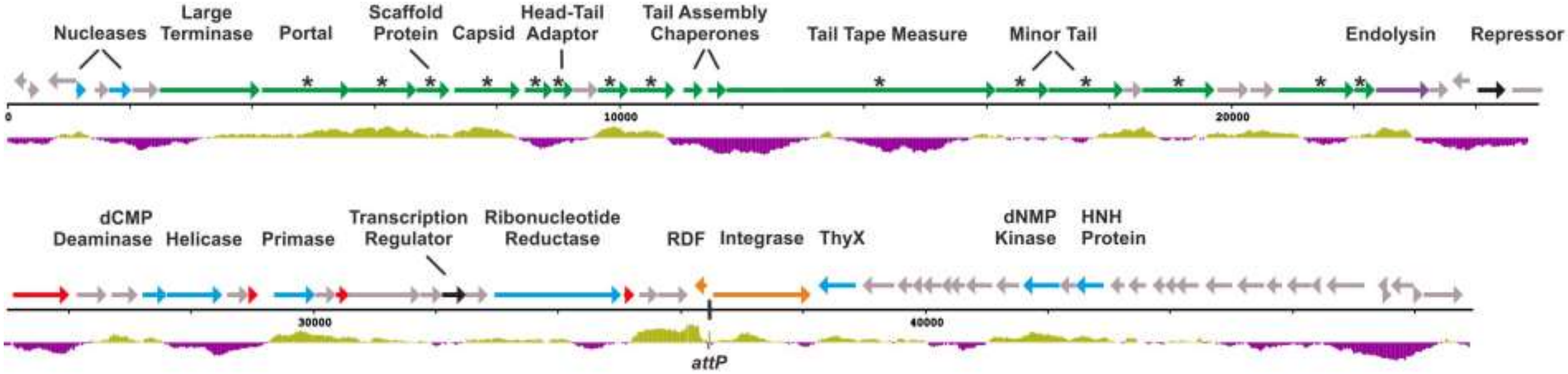

731 **Figure 3: Circos plot of the ϕJoe genome versus nine related phages.**

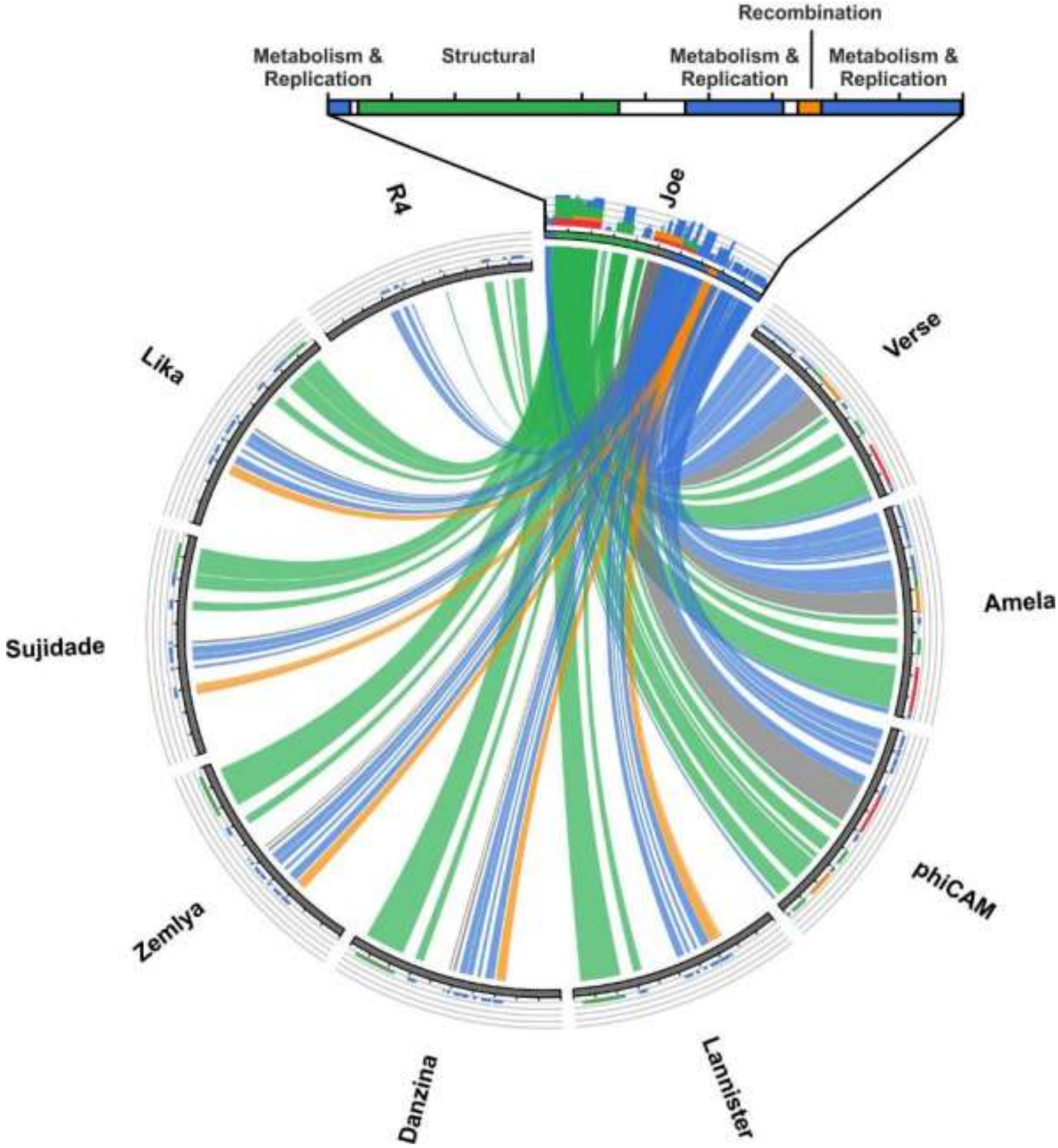

Figure 4: ϕJoe attachment sites and integration sites.

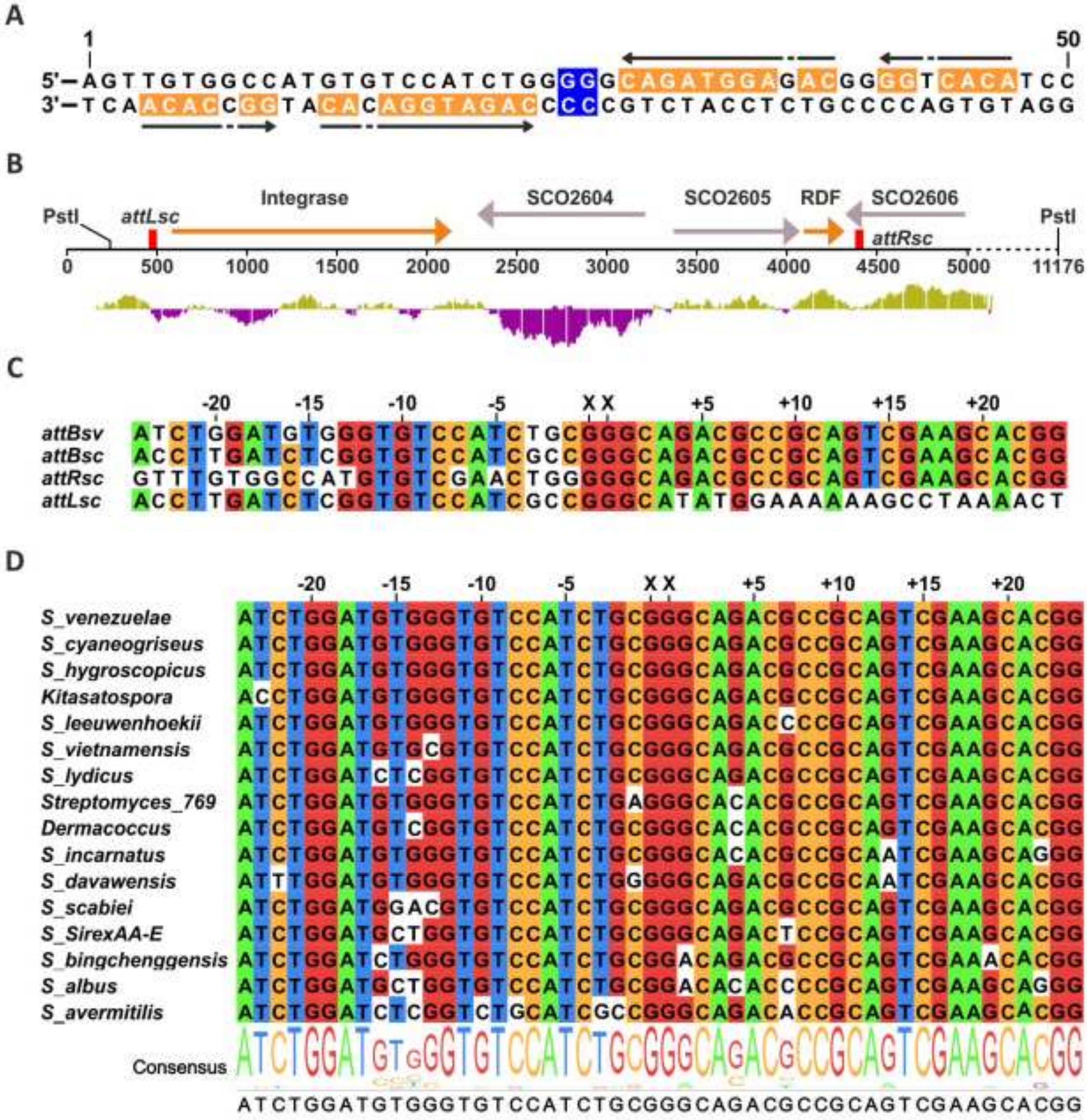

Figure 5: Activity of ϕJoe integrase in vivo and in vitro.

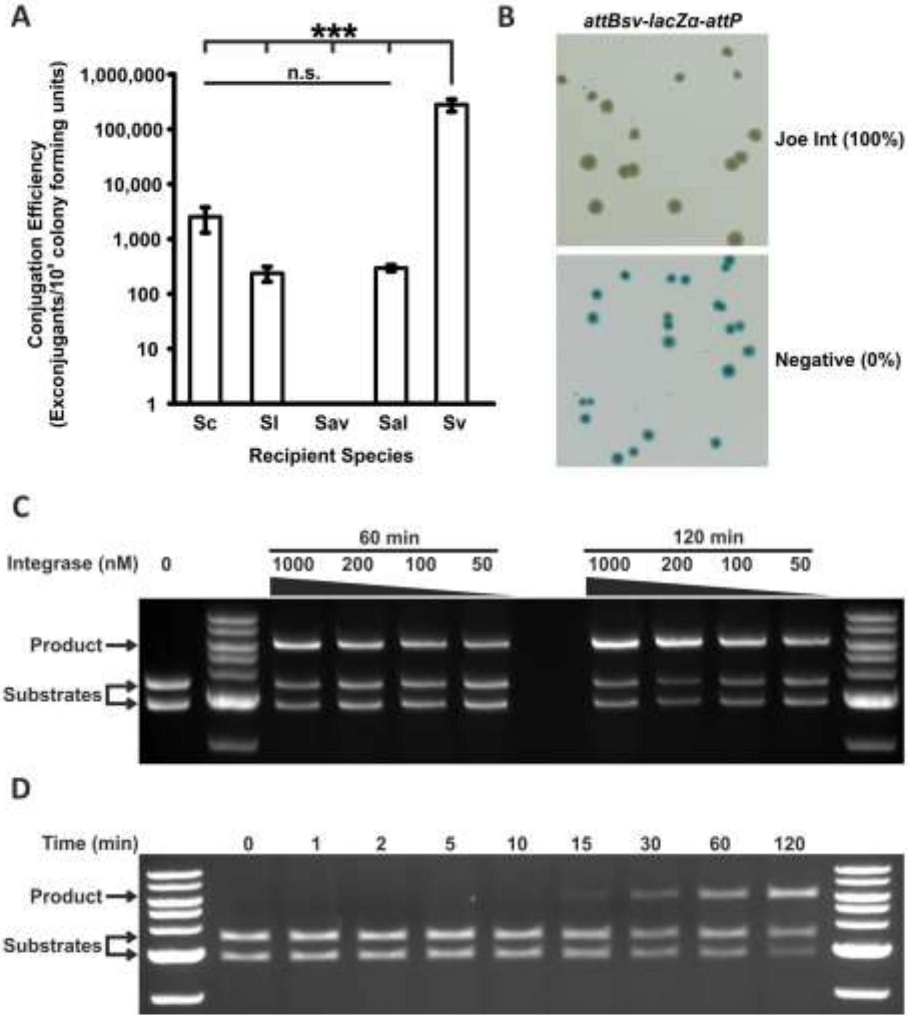

Figure 6: Identification of the ϕJoe RDF, gp52.

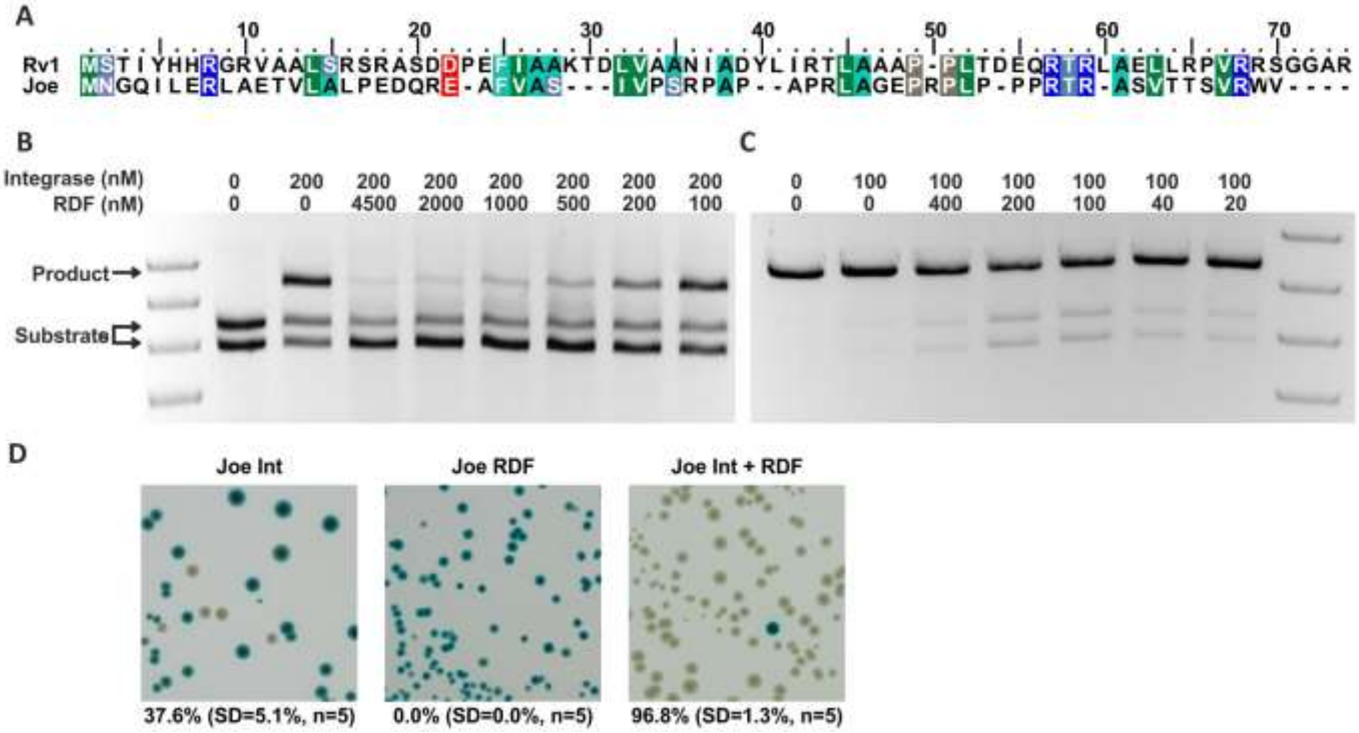

Figure Legends.

Figure 1: A ϕJoe virion imaged by transmission electron microscopy. Viral particles were negatively stained with uranyl acetate and this image was taken at 220,000x magnification. The scale bar represents 100 nm.

Figure 2: Schematic of the ϕJoe genome. The genome is 48,941 bp in length. ORFs were predicted using GeneMark and Glimmer then manually curated. ORFs are labelled and colour-coded based on their predicted function. Orange = recombination; cyan = metabolism and DNA processing/replication; green = structural proteins; purple = lysis; black = regulatory; grey = hypothetical proteins with no known function; red = candidate RDF genes. Genes marked with an asterisk encode structural proteins that were detected by tandem MS:MS. The histogram below the genome contains purple bars to indicate below-average GC content (65.5%) and green bars to indicate above-average GC content (1000 nt window size, 20 nt step).

Figure 3: Circos plot of the ϕJoe genome versus nine related phages. A Blastn comparison was carried out for ϕJoe, the five sequenced phage with a ϕJoe-like integrase, the three closest whole genome matches and the well-characterized R4 phage. The E-value cut-off was set to $1x10^{-100}$ and the HSPs to 100, ribbons are coloured by genomic regions as defined in Figure 1 and depicted above the Circos plot. The histograms above each genome are coloured to reflect relative homology to the ϕJoe sequence based on Blast score (Red>Orange>Green>Blue).

Figure 4: ϕJoe attachment sites and integration sites. A. Diagram of ϕJoe *attP* showing the central dinucleotides (Purple) and imperfect inverted repeats (Orange and arrows). **B.** Schematic of the genomic context of the two *S. coelicolor* integration sites (*attLsc* and *attRsc*, red boxes) used by the ϕJoe integrating plasmid pCMF92. The location of the PstI sites used for identification of the *att* sites are shown. The DNA between the *attLsc* and *attRsc* sites is an apparent mobile genetic element with homologous integrase and RDF genes (orange arrows) to those of ϕJoe. **C.** Alignment of *S. venezuelae attB* (*attBsv*) with the two *S. coelicolor att sites* (*attRsc* and *attLsc*) and the reconstituted *attB* site (*attBsc*) that would be produced by excision of the DNA between *attRsc* and *attLsc*. **D.** Alignment of closely related *attB* sites identified by a Blastn search against the non-redundant Genbank database. Hits were first filtered for matches of at least 80% and then for an e-value of $<1x10^{10}$ and a bit score >75. Nucleotide positions in C and D are shown as distance from the crossover dinucleotides (**XX**).

Figure 5: Activity of ϕJoe integrase *in vivo* and *in vitro*. A. Conjugation efficiency of an integrating vector, containing ϕJoe *int* and *attP*, into five recipient species - *Streptomyces coelicolor* (**Sc**), *S. lividans* (**Sl**), *S. venezuelae* (**Sv**), *S. albus* (**Sal**) and *S. avermitilis* (**Sav**). Levels of significance for *S. venezuelae* versus all other species in a one-way ANOVA was p = <0.001 (3 asterisks), all other comparisons were non-significant (**n.s.**). Error bars are standard deviation (**Sc** n=5, **Sv** and **Sl** n=3, **Sal** and **Sav** n=2). **B.** Representative image of an *in vivo* integration assay to assess *attBsv/attP* recombination by ϕJoe integrase (pCMF107) and a negative control (pBAD-HisA). Recombination leads to deletion of an intervening *lacZα* gene and white colonies, inactivity produces blue colonies. Integration efficiency is shown in brackets (n=3). **C.** Representative image of *in vitro* recombination of two substrate plasmids, *attP* (pCMF91) and *attBsv* (pCMF95), to produce the co-integrant plasmid pCMF98. The

concentration of ϕJoe Integrase and incubation time for each reaction is indicated above the gel. **D.** Time-course for the integration reaction shown in part C.

Figure 6: Identification of the ϕJoe RDF, gp52. A. Alignment of ϕJoe and RV1 RDFs, coloured using the BLOSUM62 scheme. **B.** Representative agarose gel showing *in vitro* inhibition of integration by ϕJoe RDF. The concentration of ϕJoe Integrase and RDF for each reaction is indicated above the image. Reactions were stopped after 2 h and linearized using XhoI. **C.** Representative agarose gel showing *in vitro* excision reactions catalysed by ϕJoe Integrase and RDF. The concentration of ϕJoe Integrase and RDF for each reaction is indicated above the image. Reactions were stopped after 2 h and linearized using XhoI. **D.** *In vivo* excision assay to assess *attLsv x attRsv* recombination by ϕJoe integrase alone, ϕJoe RDF alone and ϕJoe integrase co-expressed with the RDF. Recombination leads to deletion of an intervening *lacZα* gene and white colonies, inactivity produces blue colonies. Expression from the T7 promoter successfully achieved almost complete excision activity for ϕJoe Int + RDF.

Table 1. Plasmids used in this study

Plasmid	Description	Resistance	Reference
pSET152	ϕC31 *int* + *attP* integrating vector	Apra	(65)
pEHISTEV	Expression vector, T7 promoter, C-terminal HIS6, TEV cleavage site	Kan	(66)
pETFPP_2	Expression vector; HIS6-MBP-3c Cleavage Site	Kan	(67)
pBAD-HisA	Expression vector, araBAD inducible promoter	Amp	Invitrogen
pCMF87	pEHISTEV + ϕJoe *int* (gp53)	Kan	This Study
pCMF90	pGEM7 + *S. coelicolor attRsc* (274 bp)	Amp	This Study
pCMF91	pSP72 + ϕJoe *attP* (354 bp)	Amp	This Study
pCMF92	ϕJoe int + *attP* integrating vector; pSET152	Apra	This Study
pCMF94	pGEM7 + *S. coelicolor attLsc* (419 bp)	Amp	This Study
pCMF95	pGEM7 + *S. venezuelae attBsv* (462 bp)	Amp	This Study
pCMF96	pETFPP_2 + ϕJoe MBP-RDF (gp52)	Kan	This Study
pCMF97	pGEM7 + *S. coelicolor* reconstituted *attBsc* (152 bp)	Amp	This Study
pCMF98	ϕJoe *attLsv*/*attRsv*; pCMF91 integrated into pCMF95	Amp	This Study
pCMF100	pEHISTEV + ϕJoe RDF	Kan	This Study
pCMF103	pACYC184 + ϕJoe *attLsv-lacZα-attRsv*	Cm	This Study
pCMF107	pBAD + ϕJoe *int*	Amp	This Study
pCMF108	pBAD + ϕJoe RDF + *int* co-expression	Amp	This Study
pCMF116	pACYC184 + ϕJoe *attBsv-lacZα-attP*	Cm	This Study
pCMF117	pEHISTEV + ϕJoe RDF + *int* co-expression	Kan	This Study
pGEM7	General cloning vector	Amp	Promega
pSP72	General cloning vector; Accession X65332	Amp	Promega
pACYC184	General cloning vector; Accession X06403	Cm	(68)
pUZ8002	Conjugation helper plasmid; RK2 derivative with defective oriT	Kan	(69)

Table 2. Primers used in this study

Primer	Sequence (5’ – 3’)
Joe Int-*attP* F	CCGTCGACCTGCAGGCATGCCGTTCCCGCAGGTCAGAGC
Joe Int-*attP* R	ACATGATTACGAATTCTGTGGATCAGAACGTCTCGG
Joe H6-Int F	TTTCAGGGCGCCATGATGAGTAACCGACTACATG
Joe H6-Int R	CCGATATCAGCCATGTCAGAACGTCTCGGCGAAG
Joe *attP* F	TACCGAGCTCGAATTAAGACCGTCTCAGCCAGG
Joe *attP* R	TATCATCGATGAATTTCAGTGAAGACGGACAGG
Joe *attB1* F	CCGGGGTACCGAATTTGTGACGTCAGCCACAGC
Joe *attB1* R	TAGACTCGAGGAATTGACAAGGAGTGGCTCTGG
Joe *attB2* F	CCGGGGTACCGAATTGACTGCGTGCCGTCAGCC
Joe *attB2* R	TAGACTCGAGGAATTCGTCGTGTCGTCTGTCAG
Joe *attB* Sv F	CCGGGGTACCGAATTACCAGGTGGTGGATGAGC
Joe *attB* Recon F	TAGACTCGAGGAATTACCTTGATCTCGGTGTCCATCGCCGGGCAGACGCCGCAGTCGAAGCACGG
Joe *attB* Recon R	CCGGGGTACCGAATTGACAAGGAGTGGCTCTGG
Joe MBP-gp52 F	TCCAGGGACCAGCAATGAACGGACAGATCCTGG
Joe MBP-gp52 R	TGAGGAGAAGGCGCGCTACACCCAGCGCACCGA
CleF	CGCGCCTTCTCCTCACATATGGCTAGC
CleR	TTGCTGGTCCCTGGAACAGAACTTCC
Joe H6-gp52 F	TTTCAGGGCGCCATGAACGGACAGATCCTGGAG
Joe H6-gp52 R	CCGATATCAGCCATGCTACACCCAGCGCACCGA
Joe pBAD Int F	GAGGAATTAACCATGAGTAACCGACTACATG
Joe pBAD Int R	TGAGAACCCCCCATGTCAGAACGTCTCGGCGAAG
Joe pBAD gp52 F	GAGGAATTAACCATGAACGGACAGATCCTGGAG
Joe pBAD Int Co-Ex F	AGTGGTAGGTTCCTCGCCATG
Joe pBAD gp52 R	GAGGAACCTACCACTCTACACCCAGCGCACCGA
Joe LzR F	GGGTGTCAGTGAAGTAGTTGTGGCCATGTGTCCATCTGGGGGCAGACGCCGCAGTCGAAGCACGGCGATTTCGGCCTATTGGT
Joe LzR R	CCTGCCACATGAAGCGGATGTGACCCCGTCTCCATCTGCCCGCAGATGGACACCCACATCCAGATAATACGCAAACCGCCTCT
Joe BzP F	GGGTGTCAGTGAAGTATCTGGATGTGGGTGTCCATCTGCGGGCAGACGCCGCAGTCGAAGCACGGCGATTTCGGCCTATTGGT
Joe BzP R	CCTGCCACATGAAGCGGATGTGACCCCGTCTCCATCTGCCCCCAGATGGACACATGGCCACAACTAATACGCAAACCGCCTCT
SPBc H6-sprA F	CCGATATCAGCCATGGAGTTAAAAAACATTGTT
SPBc H6-sprA R	TTTCAGGGCGCCATGCTTACTACTTTTCTTAGTGG
SPBc MBP-sprB F	TCCAGGGACCAGCAATGGAACCTTACCAACGT
SPBc MBP-sprB R	TGAGGAGAAGGCGCGAAGCTTACTCTGCCTTCC
SPBc LZR F	GGGTGTCAGTGAAGTAGTGCAGCATGTCATTAATATCAGTACAGATAAAGCTGTATATTAAGATACTTACTACATATCTACGATTTCGGCCTATTGGT
SPBc LZR R	CCTGCCACATGAAGCTGGCACCCATTGTGTTCACAGGAGATACAGCTTTTATCTGTTTTTTAAGATACTTACTACTTTTCTAATACGCAAACCGCCTCT

Table 2. ϕJoe Host Range.

Host Species	**Lysis (pfu^)**
Streptomyces albus **J1074**	$(2x10^{9})$
Streptomyces avermitilis	$(2x10^{9})$
Streptomyces coelicolor J1929	$(2x10^{8})$
Streptomyces coelicolor M145	✓
Streptomyces griseus	$(4x10^{8})$
Streptomyces lividans **TK24**	$(7x10^{7})$
Streptomyces nobilis	$(1x10^{4})$
Streptomyces scabies	$(6x10^{7})$
Streptomyces venezuelae	X
Streptomyces venezuelae VL7	X
Streptomyces venezuelae VS1	X
Streptomyces venezuelae 10712	X
Saccharopolyspora erythraea	X

^ Pfu/ml values quoted are illustrative of the relative plaquing efficiencies when challenged with the same phage stock propagated on *S. coelicolor* J1929